Analysis of energy cascade models of turbulence

R. Badii* and P. Talkner
General Energy Research Department, Paul Scherrer Institute, 5232 Villigen, Switzerland
(Received 19 January 1999)

The exponent τ_p that describes the scaling of the order-p moment of the energy dissipation field in fully developed turbulence is studied in a range which extends to negative values of p. The curve τ_p vs p and its derivative τ_p' are estimated in various ways, including a two-scale method. Predictions of recent cascade models agree with our findings, within the statistical errors, for moderately large, positive p. Evident discrepancies already appear, however, in the interval $p \in [0,1]$, and sometimes become dramatic for $p<0$. In the discussion of a class of cascade models, we present a scaling law which relates different moments to one another. [S1063-651X(99)04706-6]

PACS number(s): 47.27.Gs, 02.50.−r, 05.40.−a

I. INTRODUCTION

One of the most challenging aspects of fully developed turbulence is the so-called ''intermittency,'' a little-understood mechanism which is responsible for the anomalous scaling of local fluctuating observables. This phenomenon is usually exemplified by the statistics of the longitudinal velocity difference $d(\ell)=[\boldsymbol{v}(\boldsymbol{x}+\boldsymbol{\ell},t)-\boldsymbol{v}(\boldsymbol{x},t)]\cdot\boldsymbol{\ell}/\ell$, where $\boldsymbol{v}(\boldsymbol{x},t)$ is the velocity field of the fluid at the space-time point $(\boldsymbol{x},t)$ and $\boldsymbol{\ell}$ is a displacement vector of length ℓ. The moments $S_p(\ell)$ of the distribution of $d(\ell)$, defined as

$$S_p(\ell)\equiv\langle d^p(\ell)\rangle\sim s_p\ell^{\zeta_p}, \tag{1.1}$$

present a remarkable power-law behavior in ℓ with universal exponents ζ_p which, however, do not depend linearly on p (s_p being an ℓ-independent prefactor). This behavior is expected in an interval $(\ell_{\min},\ell_{\max})$ of ℓ values (called the ''inertial range,'' or IR), the lower extremum of which is usually identified with the Kolmogorov length and marks the beginning of the dissipative range; the upper one delimits large-scale motion at which no turbulence has yet set in.

Not only is the nonlinearity of ζ_p in contrast with Kolmogorov's first prediction [1] $\zeta_p=p/3$ (also known as K41 theory): the existence itself of an inertial range is often questionable, expecially for large p [2].

The only known result about the exponents ζ_p, apart from the obvious equality $\zeta_1=0$, is the relation [1]

$$\langle d^3(\ell)\rangle\sim\ell\langle\varepsilon(\ell)\rangle, \tag{1.2}$$

where $\varepsilon(\ell)$ is the energy dissipation averaged over a volume element of size ℓ, which implies $\zeta_3=1$, since the average $\langle\varepsilon(\ell)\rangle$ is nearly scale invariant. The scaling law (1.2) has been later conjectured [3,4] to hold more generally as

$$\langle d^p(\ell)\rangle\sim\ell^{p/3}\langle\varepsilon^{p/3}(\ell)\rangle, \tag{1.3}$$

so that the fluctuations of the velocity field are linked with those of the dissipation field (refined similarity or K62 theory). By defining energy dissipation exponents τ_p via the moments

$$M_p(\ell)\equiv\langle\varepsilon^p(\ell)\rangle\sim m_p\ell^{\tau_p} \tag{1.4}$$

(m_p being ℓ independent), this link is expressed by

$$\zeta_p=p/3+\tau_{p/3}. \tag{1.5}$$

The exponents τ_p, when plotted versus p, deviate considerably from zero, especially for large $|p|$. Indeed, the K62 model for the energy fluctuations [3,4] [based on a lognormality assumption for the variable $\varepsilon(\ell)$] yields

$$\tau_p^{(\mathrm{K62})}=-\tau_2 p(1-p)/2. \tag{1.6}$$

The exponent $\tau_2\approx-0.18$, often denoted with μ, has been estimated in various ways from experimental data [2,5,6].

While Eq. (1.6) provides a good fit to the data for $0\leqslant p\leqslant 2$, the parabolic falloff of the curve for $p>2$ is too steep. Moreover, the region $p<0$ has not been studied so far on experimental data. The main reason is presumably that moments $S_p(\ell)$ with negative p (actually, with any $p\notin\mathbb{N}$) cannot be computed for the velocity field, since the velocity differences take on both signs, and τ_p has often been seen mainly as a correction to the velocity scaling exponents ζ_p [7].

On the other hand, it has been long recognized that ε constitutes a field in its own right, with peculiar fluctuation properties, the nature of which is, in principle, distinct from that of the velocity fluctuations. In fact, $d(\ell)$ is an inertial-range quantity, while $\varepsilon(\ell)$ is a dissipation-range quantity [8,9], since its definition

$$\varepsilon(\ell)=\frac{2\nu}{|B|}\int_B\sum_{ij}S_{ij}(\boldsymbol{x})S_{ji}(\boldsymbol{x})\,dV \tag{1.7}$$

involves gradients of the velocity through the symmetric part $S_{ij}=(\partial v_i/\partial x_j+\partial v_j/\partial x_i)/2$ of the strain rate tensor [where the average is made over a domain $B=B(\boldsymbol{x};\ell)$, centered at $\boldsymbol{x}$ and having volume $|B|\sim\ell^3$, and ν is the kinematic viscosity].

*URL:http://www1.psi.ch/~badii

Because of its non-negative character, the quantity $\ell^3\varepsilon(\ell)$ can be assimilated to the probability $P(\ell)$ to observe a point in a volume element $B(\boldsymbol{x};\ell)$ centered at $\boldsymbol{x}$. Following this interpretation and postulating simple mechanisms for the repartition of the probability over subelements of each $B(\boldsymbol{x};\ell)$, several so-called ''cascade models'' have been elaborated (see [10–12] for a review). Moments M_p of all orders have been computed for the ε fields generated in this way, and the function τ_p has been seen as the counterpart of the generalized dimension D_p [13] which is often employed to characterize probability measures.

To our knowledge, however, analysis of experimental time series has been restricted to positive values of p only [10,12,14]. This often resulted in incomplete testing of the cascade models proposed so far. For example, a recent conjecture [15] applies a linearity assumption for τ_p, in the limit $p\to+\infty$, to a relation among moments $M_p(\ell)$ of orders p, $p+1$, and $p+2$. While improving over the lognormal prediction for $p>2$, it turns out to be inaccurate in the interval $0\leqslant p\leqslant 1$ and even dramatically diverging from the observed behavior for $p\to-\infty$, as we shall illustrate below. A modification of it [16] presents the same drawback. Other models [11,17–19] yield a function τ_p which is not defined for $p<p_0\leqslant 0$. In spite of the different physical mechanisms postulated in the derivation of the models, most τ_p curves are indeed close to the measurements for $p>1$. Investigation of the region $p<1$, however, reveals clear differences.

In this paper, we present estimates for τ_p and its derivative with respect to p, τ_p', based on Eq. (1.4) and on a two-scale method, respectively, and give evidence for a relation between moments of orders p and q which introduces a new exponent α_{pq}. We compare our findings with the predictions of various cascade models in the broadest range of p values that can be investigated with sufficient statistical reliability: this varies from $(-3,4)$ to $(-6,9)$, depending on the exponent under consideration (τ_p, τ_p', or α_{pq}).

The analysis is made on several experimental time series of different origin: they all refer to atmospheric turbulence with Taylor-Reynolds number around 10 000, except one which was recorded in a laboratory experiment dealing with a jet of dry air in air [20].

II. DIRECT ESTIMATES OF τ_p

Given a scalar velocity time series $V=\{v_1,v_2,\ldots,v_n\}$, measured by sampling the values of a velocity component in a turbulent fluid at a fixed position $\boldsymbol{x}$ and times $t_i=i\Delta t$ $(i=1,2,\ldots,n)$, the overall energy dissipation $E_i(\ell)$ in the interval $L_i=[i+1,i+\ell]$ is usually computed as [21]

$$E_i(\ell)=\sum_{j=i+1}^{i+\ell}(v_{j+k}-v_j)^2, \tag{2.1}$$

by neglecting a prefactor which depends on the viscosity ν, on the sampling time Δt, and on the increment k. The average energy dissipation in L_i is then

$$\varepsilon_i(\ell)=E_i(\ell)/\ell, \tag{2.2}$$

where the division by ℓ (rather than by ℓ^3) descends from the one-dimensional character of the time series.

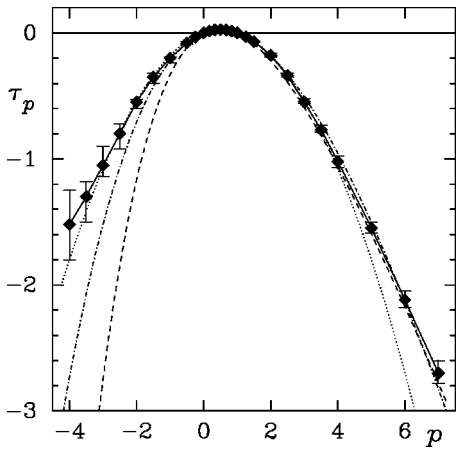

FIG. 1. Estimates of the exponent τ_p obtained from various experimental data sets (symbols joined with segments to aid the eye), compared with the curves τ_p vs p predicted from Eq. (1.6) (dotted), Eq. (5.5) (dashed), and Eq. (5.6) (dashed-dotted).

The step k appearing in the velocity difference in Eq. (2.1) controls the evaluation of the gradient and must be adjusted in dependence on Δt. Instead of a kth-neighbor differencing scheme, other approximations may be used (e.g., a parabolic fit over k consecutive points followed by an analytical derivative of the fitting curve [10]). While elaborated smoothing techniques do not improve the results substantially, an appropriate choice of k is essential, especially for large $|p|$. Too small values of k privilege instrumental and discretization noise, which unavoidably affect the signal, and short-wavelength fluctuations which have little to share with turbulence; too large values of k make the estimate of the gradient unreliable since locality is lost and the signal may even undergo a few oscillations within that interval. We have set $k\in[3,6]$ for the analysis of data sampled at 3 kHz, although values up to 12 have been considered for testing purposes.

The estimated values of the exponents τ_p are reported in Figs. 1 and 2, as well as in Table I. The figures offer a comparison with the curves τ_p versus p given by the lognormal model [Eq. (1.6)] and by the approaches of Refs. [15,16] [see, later, Eqs. (5.5] and (5.6)].

Deviations from Eq. (1.4) and dependence on k for larger $|p|$ are to be expected, although they have received little or

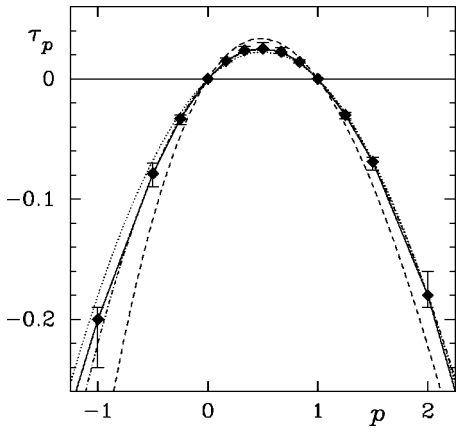

FIG. 2. Same estimates of τ_p as in Fig. 1, shown in a smaller range of p values.

TABLE I. Most reliable estimate of the exponents τ_p obtained from various experimental time series using Eq. (1.4). The error bars are reported in Fig. 1.

p	τ_p
−4	−1.52
−3.5	−1.30
−3	−1.05
−2.5	−0.80
−2	−0.55
−1.5	−0.35
−1	−0.20
−0.5	−0.079
−0.25	−0.033
0	0
1/6	0.015
1/3	0.0235
0.5	0.025
2/3	0.0225
5/6	0.014
1	0
1.25	−0.030
1.5	−0.069
2	−0.18
2.5	−0.34
3	−0.55
3.5	−0.77
4	−1.02
5	−1.55
6	−2.12
7	−2.70

no attention in the literature. Figures 3–5 illustrate three typical situations. The results are nearly independent of k, and the power law (1.4) is well verified, as long as $p \in [-0.5,2]$: notice that the values $k=10$ and 12 used in Fig. 4 are too large for a gradient evaluation. Nevertheless, except

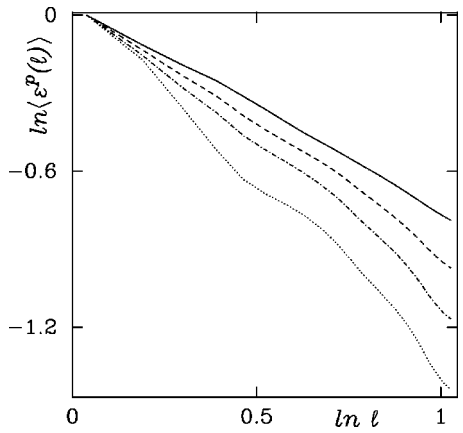

FIG. 3. Energy dissipation moment of order $p=-3$ as a function of the interval length ℓ, for various gradient-evaluation steps k: from top to bottom, $k=2$ (solid), 3 (dashed), 4 (dashed-dotted), and 6 (dotted). Logarithmic scales and arbitrary units have been used: the length ℓ varies between 60 and 585 (atmospheric data, sampled at 3 kHz).

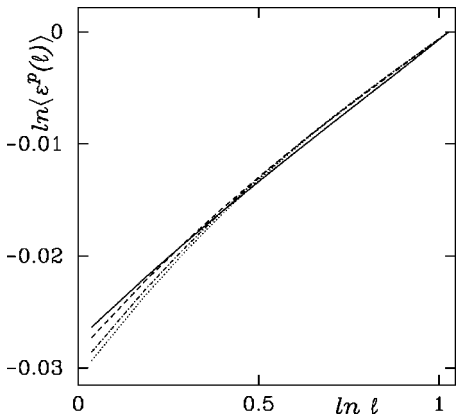

FIG. 4. Same as in Fig. 3 for $p=0.5$ and $k=2$ (solid), 6 (dashed), 10 (dashed-dotted), and 12 (dotted).

for a marked curvature for small ℓ, the corresponding curves are not far from those obtained with more appropriate k values. The uncertainty increases for increasing $|p|$: Figs. 3 and 5 show this tendency (again, a few too large k values have been used for illustrative purposes), which is more relevant for negative p.

The error bars in Figs. 1 and 2 have been drawn from the analysis of several data sets, using various values of k, and computing the slopes in the doubly logarithmic curves in different positions. The oscillations in the energy dissipation moments (1.4) as a function of ℓ, appearing for $p \ll -1$, are a sign of ''lacunarity'' [22]: the quantity $E_i(\ell)$, Eq. (2.1), grows nearly stepwise with ℓ (see Fig. 6), with steps varying in a wide range. In exactly self-affine signals, this yields prefactors to the power laws which consist of periodic functions of $\ln\ell$ [23,24]. A similar phenomenon can occur in certain sets of random points [11]. The two main slopes that can be seen in Fig. 5 for $p=4$ might also reflect lacunarity, the periodicity of which, however, largely exceeds the inertial range: the latter, therefore, is poorly defined for $p \gg 1$. For $k<-3$, instead, two oscillation periods are recognizable. The initial slope has been chosen for the estimates of τ_p: both its spread and the second slope contribute to the error bars.

While a comparison between estimated τ_p and model predictions will be made in the next section, we remark here that the K62 theory (1.6) is quite accurate for $p \leqslant 2$, as seen

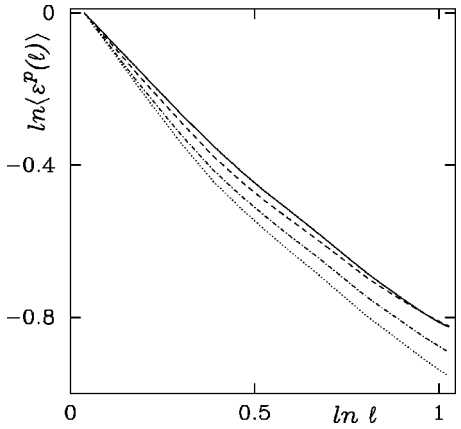

FIG. 5. Same as in Fig. 4 for $p=4$.

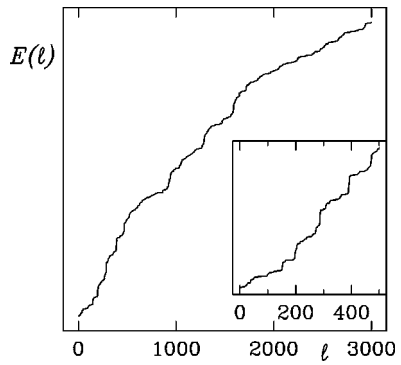

FIG. 6. Typical plot of the energy dissipation rate $E(\ell)$, Eq. (2.1), integrated over an interval of length ℓ, as a function of ℓ. A step $k=5$ was used for the evaluation of the gradients. The inlet shows an enlargement of the first portion of the main curve (atmospheric data sampled at 3 kHz).

in Figs. 1 and 2, except for the two leftmost points ($p=-3.5$ and $p=-4$). Although these might mark the onset of an asymptotic linear behavior, their high values are in part connected with the difficulty of the data analysis for $p \ll -1$: in that limit, in fact, $M_p(\ell)$ approaches $[\min_i\{\varepsilon_i(\ell)\}]^p$. Clearly, the estimation of the minimum requires an amount of data of sufficient size to allow exploration of the smoothest regions of the flow and a careful filtering of very short-wavelength fluctuations. Indeed, the minima of the energy fluctuations could sometimes be identified only after 6×10^6 energy values had been analyzed. As to the latter point, larger values of k do free the gradients from random fluctuations and yield steeper log-log plots (i.e., more negative τ_p). This, however, comes at the price of increased lacunarity effects and nonlocality of the gradient evaluations. To remedy this, at least in part, we have employed an alternative gradient estimation method. We first computed the maximum

$$D_j^{(k_0)} \equiv \max\{|v_{j+k}-v_j|, \;\; k=1,2,\ldots,k_0\} \tag{2.3}$$

of the velocity increments in absolute value over each interval $[j+1,j+k_0]$, for a fixed k_0 (chosen between 3 and 10), and then divided it by the value k_m of k at which the maximum is attained. The result has been squared and summed over ℓ steps as in Eq. (2.1). In this way, the effective, nearly noise-free dynamics of the flow is extracted. While a certain dependence on k_0 still persists, this is much weaker than the dependence of the conventional difference scheme on k. For instance, the log-log curves $M_p(\ell)$ vs ℓ produced by the two methods for $p=-3$ are comparable with $k_0=6$ and $k=4$, and with $k_0=9$ and $k=6$.

Finally, we have tested the effect of the discretization of the data on the estimates. Lower precision generally does not affect exponents with $p>1$ noticeably. For $p \ll -1$, instead, it leads to smaller values of τ_p. This result, which has been verified on several data sets by reducing the precision by a factor up to 8, is to be expected, since low resolution smoothens the data thus flattening them in the vicinity of the minima of the gradients. Large gradients, selected by $p \gg 1$, are obviously less affected, since the dynamical range of the signal is sufficiently high in their neighborhood. Therefore, measurement noise and discretization errors act in the opposite direction and it is not easy to disentangle their contributions. The slight upwards bending of the τ_p curve in Fig. 1 for $p<-3$ might be attributed to noise.

III. CASCADE MODELS

The nature of the fluctuations of the energy dissipation field and, consequently, the shape of the curve τ_p are, to a large extent, still unexplained. Several models [10–12,15–19,25–27], based on quite different assumptions about the physical mechanisms of turbulence, have been proposed since the refined similarity theory [3,4]. While a complete review of cascade models lies beyond the scope of the present article, we select a few of them for comparison with our results. Before doing this, it is useful to consider what can be said *a priori* about τ_p.

(1) Clearly, $\tau_0=\tau_1=0$. The former equality is true by definition; the latter can be verified by writing

$$\langle \varepsilon(\ell)\rangle = \frac{1}{N}\sum_{i=1}^{N} \varepsilon_i(\ell) = \frac{1}{N}\sum_{i=1}^{N}\frac{1}{\ell}\sum_{j=i+1}^{i+\ell} d_j^2(k),$$

where N is the length of the time series (minus k) and $d_j(k)=v_{j+k}-v_j$, and reordering the sums as

$$\langle \varepsilon(\ell)\rangle = \frac{1}{N\ell}\sum_{i=1}^{\ell}\sum_{j=i+1}^{i+N} d_j^2(k).$$

Assuming the stationarity of the velocity differences $d_j(k)$, the second sum converges to $N\langle d^2(k)\rangle$, which is independent of ℓ: hence, $\langle \varepsilon(\ell)\rangle$ itself is independent of ℓ and $\tau_1=0$.

(2) Furthermore, inspection of the experimental data immediately reveals that $\tau_p \neq 0$, because $E_i(\ell)$ [Eq. (2.1)] generally does not increase linearly in ℓ but rather resembles a devil's staircase, as shown in Fig. 6.

(3) The asymptotic behavior of τ_p for $|p|\to\infty$ is linear in p. In fact, for $p\to+\infty$ $(-\infty)$, $\langle \varepsilon^p(\ell)\rangle \to \varepsilon^p_{\max}(\ell)$ $[\varepsilon^p_{\min}(\ell)]$. Since the bases of these exponentials are independent of p, Eq. (1.4) implies that $\tau_p \sim c_{\pm} p$ for $p \to \pm\infty$.

(4) Bounds for τ_p have been deduced [17] under the hypothesis that

$$\langle [\varepsilon(r\ell)/\varepsilon(\ell)]^p\rangle \sim r^{\tau_p}, \tag{3.1}$$

where the energy dissipations in the ratio are computed over nested intervals of lengths $r\ell$ and ℓ $(0 \leqslant r \leqslant 1)$. Notice that three assumptions are implied here: namely, that the scaling behavior is a pure power law in r, that the exponent τ_p is the same as in Eq. (1.4), and that this holds independently of any shift of the inner interval relative to the outer one. Then, $-1<\tau_2<0$, $\tau_{p+h}-\tau_p \geqslant -h$ for $h \geqslant 0$, and $\tau_p \geqslant \tau_2+2-p$ for $p \geqslant 2$. None of these inequalities is critical: i.e., they are all widely satisfied.

(5) Under the same hypothesis, Novikov has shown [28] that $\tau_p/p \to -1$, in the limit $p\to+\infty$, if the probability distribution $W(q_{r,\ell})$ of the so-called ''breakdown coefficients'' $q_{r,\ell}=\varepsilon(r\ell)/\varepsilon(\ell)$ has no gap, as appears to be the case from the experiments.

As expected from the simplicity of the assumption supporting it, the lognormal model (1.6) cannot be correct [17,29]: indeed, it does not fulfill conditions (3)–(5). Nevertheless, it is surprisingly accurate in the interval $p \in (-2,3)$, as seen in Figs. 1 and 2. The quadratic decrease predicted for τ_p at large $|p|$ is the major source of discrepancy with the experimental values.

In order to overcome the drawbacks of this model, several alternatives have been proposed. Among the most recent ones, we mention those of Refs. [15], [16], which we study in the next sections, and of Refs. [28], [18], which are only applicable for p larger than some p_0, referring the reader to [10,12,30] for older models.

The several expressions proposed for τ_p arise from quite disparate physical motivations: a first group has its roots in self-similar constructions of fractal probability measures [22,25,31–34]; a second one in assumptions about the shape of the distribution $W(q_{r,\ell})$ of the breakdown coefficients [11,19,27,28]; a third combines assumptions about the asymptotic behavior of τ_p for $p \to +\infty$ with scaling laws which relate moments M_p [Eq. (1.4)] of different orders p with one another [15,16], rather than M_p with the length scale ℓ.

In Ref. [15], She and Lévêque (SL) have conjectured that $\lim_{p\to+\infty} \tau_p/p = -2/3$; Novikov [28] has questioned this value, suggesting replacing it with -1 [see point (5) above]. This proposal has been received by Chen and Cao (CC) in Ref. [16] and incorporated in the scheme of Ref. [15]. The two curves τ_p vs p corresponding to these choices (to be discussed in Sec. V) are also plotted in Figs. 1 and 2: the value $\tau_2 = -0.18$ has been used. They agree quite well with the experimental results for $p>2$, with a slight preference for SL for $p>5$ and a clear superiority of CC for $-0.5 \leqslant p \leqslant 5$ (SL being inaccurate already for $p<2$).

The better performance of SL for larger p does not imply, however, that the $-2/3$ assumption for the limit slope is correct: in fact, we have chosen not to consider values of p above 7 because of the unreliability of the estimates, notwithstanding the high quality of the data. Simply, the asymptotic regime might set in for still higher p, so that it would not be visible from these plots. On the other hand, the value -1 for the slope at $+\infty$ might also be incorrect, despite the apparently convincing argumentation of Ref. [28]: indeed, although the distribution $W(q_{r,\ell})$ exhibits no noticeable gap, the scaling exponent of the breakdown coefficients [see Eq. (3.1)] need not equal τ_p exactly.

While our results cannot resolve the question of τ_p's limit for $p \to +\infty$, they definitely show the inadequacy of both SL and CC for negative p (not to mention other models which are not defined below some $p_0 \leqslant 0$). If the lognormal approach yields too steep a descent (quadratic in p), these models predict an even steeper one (exponential). Our results, although not extending below $p=-4$ and affected by a slight upward bend of the τ_p curve, point to a linear decrease of τ_p for $p \to -\infty$, in agreement with our conjecture (3) above.

Something is substantially wrong in the approaches [15,16] for $p<0$. Before analyzing them, we present the results of an independent method for the evaluation of the derivative τ_p' of τ_p with respect to p, since this is related to the SL-CC scheme.

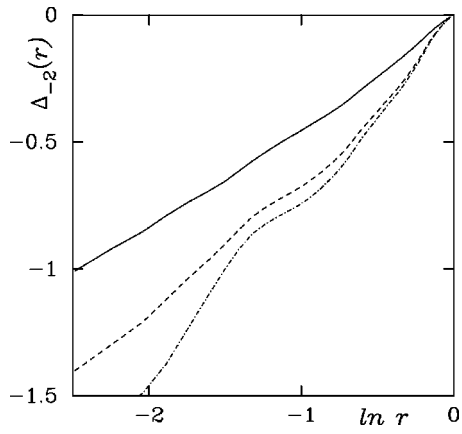

FIG. 7. Two-scale difference $\Delta_p(r)$ of the moment derivatives of order $p=-2$ versus ln$r$ computed from atmospheric data, using $k=3$, 5, and 7 from top to bottom (i.e., solid, dashed, and dashed-dotted line, respectively).

IV. TWO-SCALE ESTIMATES OF τ_p'

The derivative $\tau_p' = d\tau_p/dp$ can be directly estimated by comparing expectations of suitable observables referring to two different length scales. Following [6], we consider two time intervals having the origin in common and lengths ℓ and $\ell' = r\ell$. Setting

$$L_p(\ell) = \ln\langle \varepsilon^p(\ell)\rangle \tag{4.1}$$

and recalling Eq. (1.4), the derivative of L_p with respect to p can be written as

$$L_p'(\ell) = \langle \varepsilon^p \ln \varepsilon\rangle / \langle \varepsilon^p\rangle \sim m_p'/m_p + \tau_p' \ln \ell, \tag{4.2}$$

where $m_p' = dm/dp$ is the derivative of the prefactor in Eq. (1.4). Computing L_p' across the two time intervals permits writing the difference as

$$\Delta_p(r) \equiv L_p'(\ell') - L_p'(\ell) \sim \tau_p' \ln r, \tag{4.3}$$

where the prefactors disappear because of the common origin of the intervals. Notice, however, that no deviation of relation (1.4) from a pure power law (e.g., a logarithmic dependence on ℓ) is assumed here.

Two typical sets of curves $\Delta_p(r)$ vs ln$r$ are displayed in Figs. 7 and 8, for $p=-2$ and 3, respectively. Deviations from linearity and dependence on step k for the evaluation of the gradients are evident, especially for $p=-2$. The error bars in Fig. 9, which shows the estimated curve τ_p' vs p, account for this. For smaller $|p|$, such effects are negligible and the estimates are extremely accurate and consistent throughout several data sets.

Comparison with the expression of τ_p' given by the lognormal formula (1.6) and by the SL and CC approximations [Eqs. (5.5) and (5.6), respectively] shows that the latter behaves like an improvement over a linear fit (lognormal) which extends the accuracy from the interval [0,2] to the interval $[-2,4]$. The SL formula, instead, fails to fit the data in the whole displayed range. This is particularly striking in the interval [0,1] (see also Fig. 2), especially if compared

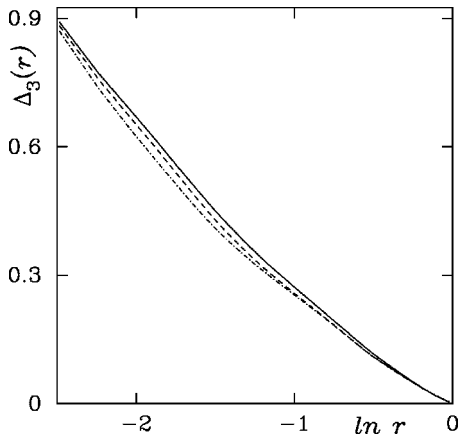

FIG. 8. Same as in Fig. 7 for $p=3$.

with the agreement for larger p values. Moreover, neither SL nor CC are able to reproduce the experiment for small p ($p<0$ and $p<-2$, respectively).

It should be noted that the values of τ_p' estimated with this method for $p<-1$ are definitely larger than those obtained by numerically differentiating the curve τ_p vs p obtained from Eq. (1.4) and displayed in Figs. 1 and 2. Despite the large error bars, a bending toward a constant value, as conjectured in Sec. III, is already apparent for $p<-2$. No precise value can be identified, however. It has not been possible to push these estimates reliably to the right of $p\approx 4$ because of the emergence of a second slope in the plots of $\Delta_p(r)$ vs $\ln r$.

It must be remarked that the value of ℓ is an additional free parameter which could be varied to improve the quality of the results. No systematic investigation has been made so far: for the atmospheric data sampled at 3 kHz, we have used $\ell=600$.

V. BEYOND THE INERTIAL RANGE

The inability of the SL and CC approximations (5.5) and (5.6) to reproduce the experimental results for negative p requires a careful investigation of their derivation. These models stem from the wish to obtain scaling laws which hold in a broader range than Eq. (1.4) and present smaller deviations from the proposed behavior, so as to facilitate defining an ''inertial range.''

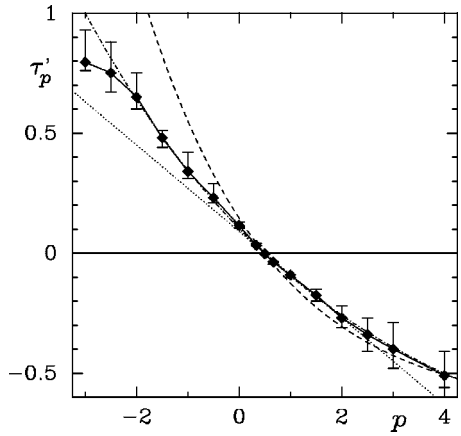

FIG. 9. Derivative τ_p' of τ_p versus p, compared with the predictions of Eq. (1.6) (dotted), Eq. (5.5) (dashed), and Eq. (5.6) (dashed-dotted).

When working with velocity differences, this is usually identified with an interval $(\ell_{\min},\ell_{\max})$ of length scales in which the pure power law (1.1) is well verified. In particular, it is customary to refer to the case $p=3$, although the extrema $\ell_{\min}$ and $\ell_{\max}$ depend on p. This procedure, unfortunately, is only successful at high Reynolds number (commonly denoted by $R=V\ell_{\max}/\nu$, where V is a typical velocity at the ''integral'' scale $\ell_{\max}$): in Ref. [35], for example, only for $R>47\,000$ could a power law be detected in some range for $p=2$, 3, and 6. For $\ell<\ell_{\min}$, the moments exhibit a different behavior, not necessarily of a power-law type.

A further difficulty arises with the so-called ''odd moments,'' i.e., moments S_p having an odd value of the exponent p: the sign fluctuations of the velocity differences often make the estimate of ζ_p quite unreliable. In order to reduce the ''invasion'' of the dissipation range and overcome the odd-moment problem, the scaling relation

$$\langle|d(\ell)|^p\rangle\sim w_p\langle|d(\ell)|^3\rangle^{\zeta_p^*} \tag{5.1}$$

is often used, where w_p does not depend on ℓ. The length scale ℓ, which was the independent variable in Eq. (1.1), is replaced by the third moment S_3^* of the velocity differences (in absolute value) by analogy with Eq. (1.2). This substitution, called ''extended self-similarity'' (ESS), was proposed in Ref. [35] with the same exponent ζ_p as in Eq. (1.1): actually, the ESS exponent ζ_p^* is not necessarily the same as ζ_p [2]. The ESS is an example of a ''relative'' scaling law: i.e., it may be used to infer the value of an exponent starting from a given one (ζ_3^* in this case).

The SL and CC models borrow this idea and apply it to the energy dissipation moments (1.4). In Ref. [15], the ratio

$$R_{p+1}(\ell)=\frac{M_{p+1}(\ell)}{M_p(\ell)} \tag{5.2}$$

is assumed to depend on its ''predecessor'' $R_p(\ell)$ as

$$R_{p+1}(\ell)\sim A_pC(\ell)R_p^{\beta}(\ell), \tag{5.3}$$

with β a constant, independent of p. The prefactor consists of two parts. The former, A_p, is a function of p only. The latter, $C(\ell)$, was written as $R_\infty^{1-\beta}(\ell)$, where

$$R_\infty(\ell)=\lim_{p\to\infty}R_p(\ell)$$

accounted for the ''most intermittent structures'' of the fluid. Dimensional arguments, tied to the supposed filamentary nature of these structures, led to the assumption [15]

$$R_\infty(\ell)\sim\ell^{-2/3}, \tag{5.4}$$

which implies the SL formula

$$\tau_p^{(\mathrm{SL})} = -\frac{2}{3}p + 2\left[1 - \left(\frac{2}{3}\right)^p\right], \tag{5.5}$$

in the derivation of which τ_0 and τ_1 were set to 0. The only difference in the CC approach is its acceptance of Novikov's criticism [28], which demands replacing the value 2/3 in Eq. (5.4) with 1: the corresponding formula reads

$$\tau_p^{(\mathrm{CC})} = -p + [(1+\tau_2)^p - 1]/\tau_2 . \tag{5.6}$$

A few remarks are in order. First, the disagreement for $p < 0$ should not come as a surprise, since the above expressions were deduced by ''fixing'' the scaling with an assumption at $p \to +\infty$ only, ignoring the range $p < 0$; moreover, dimensional arguments were invoked, analogously to Kolmogorov's 1941 approach [1], which fails to describe the deviations of the exponents from linearity. Secondly, the law (5.3) is arbitrarily restricted to integer values of p: in fact, since ε is non-negative, one could consider moments of orders $p-h$, p, and $p+h$, with p and $h \in \mathbb{R}$. This would make it clear that the SL-CC scheme is basically an assumption about τ_p' for $p \to +\infty$ ($\tau_{p+1} - \tau_p$ goes over to τ_p' in such a limit). As seen in the preceding section, τ_p' can be estimated directly and the results agree much better with the CC formula than with SL's, in the chosen p range.

The third and most important point is that relation (5.3) is not well satisfied as long as the ℓ-dependent prefactor $C(\ell)$ is included, no matter which value is taken (2/3 or 1) for the scaling exponent in Eq. (5.4). Indeed, the influence of the scaling exponent at $p = +\infty$ should be stronger for large p and weaker for small p, whereas fixed contributions are assumed in Eq. (5.3). We have verified this for several values of p and data sets. A better scaling is obtained by plotting R_{p+1} versus R_p, without any ℓ-dependent correction. As a consequence, relation (5.3) must be rewritten as

$$R_{p+1}(\ell) \sim R_p^{\beta_p}(\ell), \tag{5.7}$$

where the exponent β_p is explicitly a function of p. This is quite obvious since, for example, relation (5.7) reduces to an identity in the limit $p \to \infty$, where the increment 1 is negligible with respect to p and $\beta_p \to 1^+$. The same observation can be immediately made by taking R_{p+h}, instead of R_{p+1}, with $0 < h \ll 1$. Using Eq. (1.4), it is readily seen that

$$\beta_p = \frac{\tau_{p+1} - \tau_p}{\tau_p - \tau_{p-1}}. \tag{5.8}$$

The values of β_p estimated from our data are plotted in Fig. 10, together with the curves β_p vs p that are obtained by substituting Eqs. (1.6) and (5.5) into Eq. (5.8). As expected, the experimental data are better reproduced by the SL formula for $p > 0$ and by the lognormal prediction for $p < 0$. The limits for $|p| \to \infty$ converge quite neatly to 1, as predicted [a good fit is given by $\beta_p \approx 0.75/(p-1)+1$]. The vertical asymptote at $p = 1$ comes from the SL choice of taking an increment of 1 in p in Eq. (5.3), which we have respected in Eq. (5.7). As already remarked, there is no special reason for doing so: any real increment h is equally legitimate.

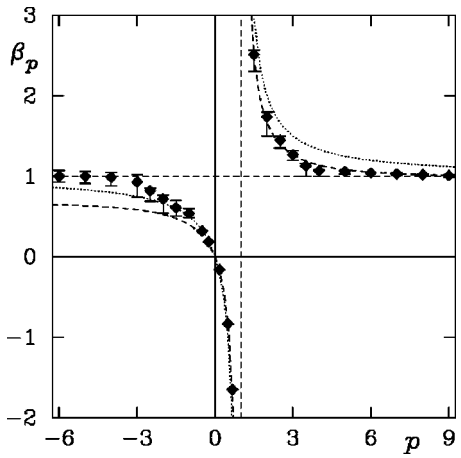

FIG. 10. Scaling exponent β_p of Eq. (5.7) versus p, compared with its analytic expression as given by Eq. (1.6) (dotted) and Eq. (5.5) (dashed).

Two typical plots of R_{p+1} vs R_p are shown in Fig. 11: the scaling law (5.7) holds, except for some oscillations for $p \ll -1$. Using Eq. (5.3) with Eq. (5.4) usually yields a curvature which makes a linear fit (in a doubly logarithmic scale) hard.

Finally, we have investigated a simpler scaling law involving the order-p moment M_p of Eq. (1.4), namely,

$$M_p(\ell) \sim M_q^{\alpha_{pq}}(\ell), \tag{5.9}$$

which we have verified in the case $q = p-1$, for comparison with Eq. (5.7), although this relation holds much more generally. The estimated values of α_{pq}, with $q = p-1$, are reported in Fig. 12, together with the expressions obtained from Eqs. (1.6) and (5.5): in fact, it is easy to see that

$$\alpha_{p+1,p} = \tau_{p+1}/\tau_p . \tag{5.10}$$

Two curves illustrating Eq. (5.9) are shown in Fig. 13. The same remarks apply as those made previously for Figs. 10 and 11, except that the new scaling law (5.9) is satisfied

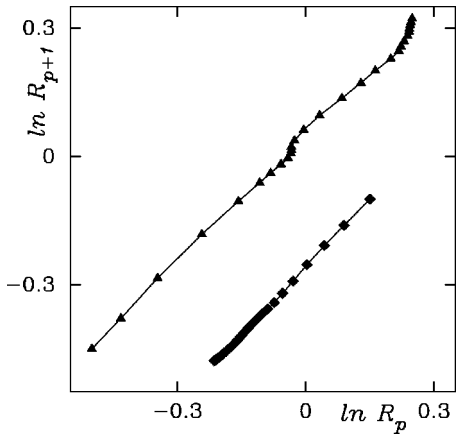

FIG. 11. Ratio R_{p+1} versus R_p, Eq. (5.2), in a log-log plot, computed from atmospheric data for $p = -3$ (upper curve, triagles) and $p = 4$ (lower curve, squares). The curves have been shifted to avoid overlapping.

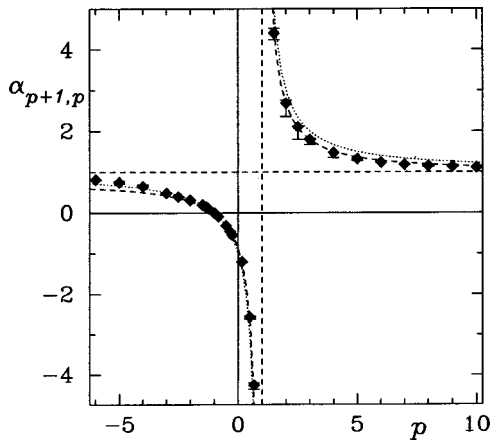

FIG. 12. Scaling exponent $\alpha_{p+1,p}$ of Eq. (5.10) versus p, compared with its analytic expression as given by Eq. (1.6) (dotted) and Eq. (5.5) (dashed).

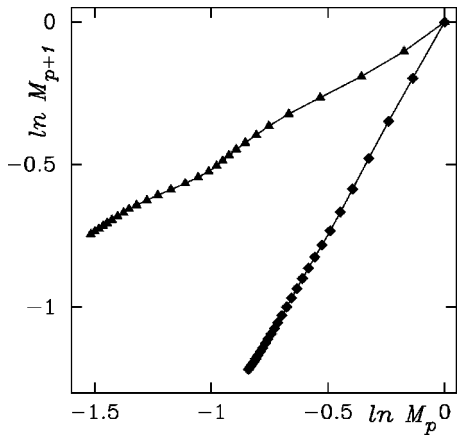

FIG. 13. Doubly logarithmic plot of moment M_{p+1} versus moment M_p, illustrating Eq. (5.7), computed from atmospheric data for $p=-3$ (upper curve, triangles) and $p=4$ (lower curve, squares).

much more accurately than Eq. (5.7) or Eq. (5.3): the estimated values of α are, correspondingly, more precise than those of β_p.

The power law (5.9) holds extremely well in a broad range of ℓ values, even around the extrema where a definite bending is exhibited by the moments $M_p(\ell)$ vs ℓ, Eq. (1.4), for $|p|>3$. Therefore, it is tempting to use the values $\alpha_{p,p-1}$ to extrapolate values of τ_p from a known one, in the spirit of the extended self-similarity approach [35] [see Eq. (5.1)]. For instance, one could write

$$\tau_p = \tau_2 \alpha_{3,2} \alpha_{4,3} \cdots \alpha_{p,p-1},$$

or an analogous relation using $\alpha_{p,p-h}$, with $h<1$. Although this may indeed be useful for moderate values of p, the tendency of $\alpha_{p+1,p}$ to 1 for large $|p|$ makes the progress per iteration step smaller and smaller, to a point at which the cumulative estimation errors on the α's in the product dominate over the value of τ_p thus obtained. Scaling relations of the types (5.3), (5.7), and (5.9), however, are worth further investigation.

VI. CONCLUSIONS

We have studied the moments of the locally averaged energy dissipation from experimental turbulent signals in a range of exponents that includes positive and negative values. The results have been examined upon variation of various estimation parameters and compared with a two-scale method which yields the derivative of the intermittency exponent. Deficiencies of currently popular cascade models have been pointed out and some of the reasons for their partial failure have been analyzed. In this discussion, we have presented a simple scaling law which is quite well satisfied and may be used to improve the quality of the estimates of the intermittency exponents. Further investigation on the gradient-evaluation methods, on Novikov's breakdown coefficients, and on the new scaling law is in progress.

ACKNOWLEDGMENTS

We gratefully acknowledge receiving data from M. Furger, J. Peinke, and R.O. Weber.

[1] A.N. Kolmogorov, Dokl. Akad. Nauk SSSR **30**, 301 (1941).
[2] A. Arneodo *et al.*, Europhys. Lett. **34**, 411 (1996).
[3] A.M. Obukhov, J. Fluid Mech. **13**, 77 (1962).
[4] A.N. Kolmogorov, J. Fluid Mech. **13**, 82 (1962).
[5] F. Anselmet, Y. Gagne, E.J. Hopfinger, and R. Antonia, J. Fluid Mech. **140**, 63 (1984).
[6] R. Badii and P. Talkner, Europhys. Lett. **43**, 284 (1998).
[7] In order to allow for noninteger, positive values of p, the alternative expression $S_p^*(\ell)=\langle|d(\ell)|^p\rangle\sim\ell^{\zeta_p^*}$ is sometimes considered [2]: the asterisk is a reminder that the value of the exponent may be different than in Eq. (1.1). Indeed, $\zeta_1^*\neq 0$, which agrees with Eq. (1.5), since $\tau_{1/3}\neq -1/3$: notice that $\zeta_1=0$ is, instead, in contrast with Eq. (1.5).
[8] E. Bacry, A. Arneodo, U. Frisch, Y. Gagne, and E.J. Hopfinger, in *Turbulence and Coherent Structures*, edited by O. Metais and M. Lesieur (Kluwer, Dordrecht, 1991), p. 203.
[9] S. Grossmann and D. Lohse, Europhys. Lett. **21**, 201 (1993).
[10] C. Meneveau and K.R. Sreenivasan, J. Fluid Mech. **224**, 429 (1991).
[11] E.A. Novikov, Phys. Fluids A **2**, 814 (1990).
[12] U. Frisch, *Turbulence: The Legacy of A.N. Kolmogorov* (Cambridge University Press, Cambridge, England, 1995).
[13] A. Renyi, *Probability Theory*, North-Holland, Amsterdam, 1970).
[14] S. Chen, K.R. Sreenivasan, and M. Nelkin, Phys. Rev. Lett. **79**, 1253 (1997).
[15] Z.S. She and E. Lévêque, Phys. Rev. Lett. **72**, 336 (1994).
[16] S. Chen and N. Cao, Phys. Rev. E **52**, 5757 (1995).
[17] E.A. Novikov, Appl. Math. Mech. (in Chinese) **35**, 231 (1971).
[18] M. Nelkin, Phys. Rev. E **52**, 4610 (1995).
[19] Y. Saito, J. Phys. Soc. Jpn. **61**, 403 (1992).
[20] The atmospheric data consist of wind velocity recorded at a

height of 25 m above ground, with a sampling frequency between 2 and 30 kHz, using a hot-film anemometer with a spatial resolution of 2 mm (M. Furger and R.O. Weber, Paul Scherrer Institute, Switzerland). The average and rms velocities range between 1.5 and 4 m/s, the integral length is about 100 m, the Kolmogorov length 0.45 mm, and the Taylor-Reynolds number 10 000. The laboratory data refer to air velocity in an axisymmetric free jet (dry air in air), recorded at 8 kHz with a hot-wire anemometer (resolution 1 mm) placed at a distance of 125 nozzle diameters from the source, along the axis of the jet (Ch. Renner, J. Peinke, University of Bayreuth, Germany). The Reynolds number at the nozzle was 27 000. At the probe, the mean velocity was 2.25 m/s, the integral length 67 mm, the Kolmogorov length 0.25 mm, and the Taylor-Reynolds number 200. Each set contains 10^7 points. We recall that the kinematic viscosity in air has the value $\nu = 1.56 \times 10^{-5}$ $m^2\,sec^{-1}$.

[21] Temporal displacements at a fixed position are equivalent to spatial displacements at a fixed time by Taylor's hypothesis: see G.I. Taylor, Proc. R. Soc. London, Ser. A **164**, 476 (1938). Therefore, the symbol $\not\ell$ will denote temporal displacements in the discussion of the data analysis.

[22] B.B. Mandelbrot, *The Fractal Geometry of Nature* (Freeman, San Francisco, 1982).

[23] R. Badii and A. Politi, Phys. Lett. **104A**, 303 (1984).

[24] L.A. Smith, J.D. Fournier, and E.A. Spiegel, Phys. Lett. **114A**, 465 (1986).

[25] C. Meneveau and K.R. Sreenivasan, Phys. Rev. Lett. **59**, 1424 (1987).

[26] I. Hosokawa, Phys. Fluids A **1**, 186 (1989).

[27] S. Kida, J. Phys. Soc. Jpn. **60**, 5 (1991).

[28] E.A. Novikov, Phys. Rev. E **50**, 3303 (1994).

[29] B.B. Mandelbrot, in *Statistical Models of Turbulence*, edited by M. Rosenblatt and C. Van Atta, (Springer, Berlin, 1972), p. 333.

[30] T. Bohr, M.H. Jensen, G. Paladin, and A. Vulpiani, *Dynamical Systems Approach to Turbulence* (Cambridge University Press, Cambridge England, 1998).

[31] E.A. Novikov and R.W. Stewart, Izv. Akad. Nauk SSSR, Ser. Geogr. Geofiz. **3**, 245 (1964).

[32] B.B. Mandelbrot, J. Fluid Mech. **62**, 331 (1974).

[33] U. Frisch, P.L. Sulem, and M. Nelkin, J. Fluid Mech. **87**, 719 (1978).

[34] R. Benzi, G. Paladin, G. Parisi, and A. Vulpiani, J. Phys. A **17**, 3521 (1984).

[35] R. Benzi, S. Ciliberto, R. Tripiccione, C. Baudet, F. Massaioli, and S. Succi, Phys. Rev. E **48**, R29 (1993).